NANO LETTERS

Letter

pubs.acs.org/NanoLett

Ultrafast Spectroscopy of Quantum Confined States in a Single CdSe Nanowire

Thorsten Schumacher,[†,‡] Harald Giessen,[‡] and Markus Lippitz*[,†,‡]

[†]Max Planck Institute for Solid State Research, Heisenbergstrasse 1, D-70569 Stuttgart, Germany

[‡]4th Physics Institute and Research Center SCoPE, University of Stuttgart, Pfaffenwaldring 57, D-70550 Stuttgart, Germany

Supporting Information

ABSTRACT: We measure for the first time transient absorption spectra of individual CdSe nanowires with about 10 nm diameter. Confinement of the carrier wave functions leads to discrete states which can be described by a six-band effective mass model. Combining transient absorption and luminescence spectroscopy allows us to track the excitation dynamics in the visible and near-infrared spectral range. About 10% of all absorbed photons lead to an excitation of the lowest energy state. Of these excitations, less than 1% lead to a photon in the optical far-field. Almost all emission is reabsorbed by other parts of the nanowire. These findings might explain the low overall quantum efficiency of CdSe nanowires.

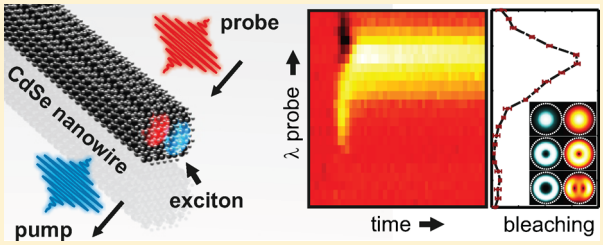

KEYWORDS: *Semiconductor nanowires, transient absorption spectroscopy, single particle spectroscopy, exciton*

Semiconductor nanowires bridge the gap between the nanoscale and the outside world.[1,2] This makes them very appealing nanosystems for fundamental research,[3,4] next generation solar cells,[5] and coupling to plasmonic nanostructures.[6−8] When the diameter of the wire comes in the range of the exciton Bohr radius, quantum confinement of the electronic states gives an additional degree of freedom to engineer the optical properties of the wire. In this size range, the steep variation of the optical response with the nanowire diameter makes single wire experiments indispensable.[9,10]

Fluorescence spectroscopy of single emitters is a well-established technique and has given valuable insight into the photophysics of nanowires.[9,11,12] Recently, ground state absorption of a single thin nanowire was determined by various techniques.[13−15] However, the picosecond dynamics of carrier relaxation before photoemission has to be investigated by nonlinear optical techniques such as transient absorption spectroscopy. As nonlinear optical signals are generally rather weak, such experiments are easier on ensembles of nanostructures.[16−19] In addition, spectral diffusion and photobleaching complicate the experiments at room temperature. Only experiments at a fixed wavelength have been published so far.[20,21] Here, we present an ultrafast transient absorption technique that allows us to track the excitation dynamics in a single CdSe nanowire of about 10 nm diameter in the visible and near-infrared spectral range.

One surprising property of semiconductor nanowires is their low luminescence quantum efficiency,[10,22−24] especially compared to their zero-dimensional analogue, namely, nanocrystals.[25,26] Using our transient absorption technique, we can determine how many carriers we excited to each state, and we can follow their fate until photoemission or radiation-less recombination occurs. Our experiment makes it clear that large parts of the emitted photons do not reach the optical far-field, that is, are reabsorbed by the nanowire itself. This is in contrast to nanocrystals, where few absorbing states are in the close environment of the emitter.

Figure 1a presents the essential idea of our experiment. A pump pulse is focused on an individual CdSe nanowire. The narrow diameter of the wire (about 10 nm) leads to quantum confined states of electrons and holes, as sketched in the ladder scheme.[13,14,27] Our near-UV pump pulse excites electrons from the valence band high into the conduction band (blue arrow). Via radiative and nonradiative processes charge carriers relax into lower energetic confined states on a picosecond time scale. The probe pulse (red arrow) interrogates the nanowire absorption as a function of time delay and probe photon energy. The key parts of our experimental setup are depicted in Figure 1b. The pump pulses are the frequency doubled output of a Ti:Sa oscillator (76 MHz repetition rate) with 150 fs pulse length, 390 nm wavelength, and 15 fJ pulse energy, where we find negligible photobleaching. The probe pulses are generated by an optical parametric oscillator. We can tune their center wavelength from 520 to 750 nm and use pulse energies of 130 fJ. Maximum absorption of the pump and probe pulses is achieved by linear polarization along the wire axis.[28−30] Amplitude modulation of the pump pulses via an acousto-optical modulator (AOM) allows us to resolve pump induced transmission changes down to 10^{-6} utilizing a lock-in technique. A mechanical delay line defines the time between

Received: January 21, 2013
Revised: March 1, 2013
Published: March 21, 2013

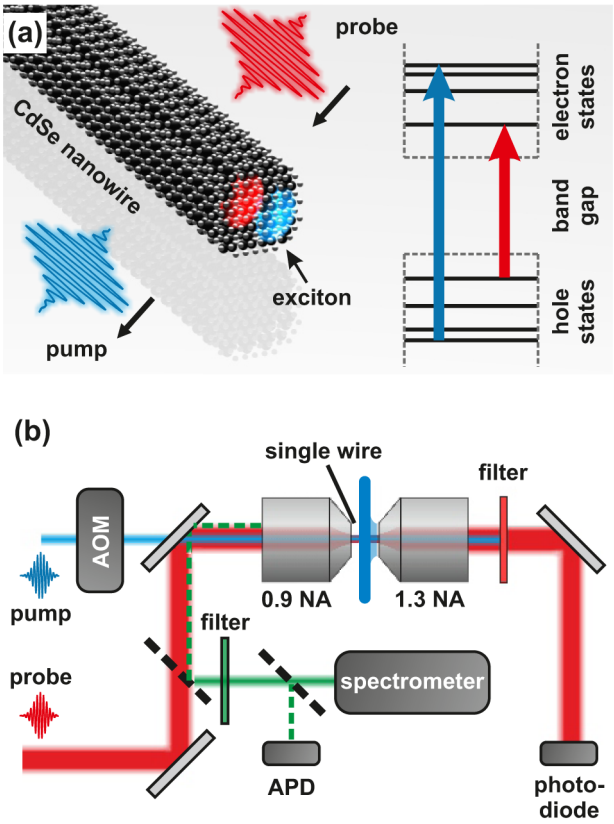

Figure 1. (a) When a near-UV pump pulse has excited a CdSe nanowire, the population of quantum-confined states changes the optical absorption that is seen by a consecutive probe pulse. The ultrafast temporal dynamics of the carriers after excitation far above the band gap (blue arrow in ladder scheme) is investigated by tuning the second pulse (red arrow) in time and energy. (b) Experimental setup for transient absorption spectroscopy. The dashed lines represent flip mirrors to switch between transient absorption and luminescence measurements. (c,d) Transmission electron microscopy images of different CdSe nanowires. (d) We observe diameter fluctuations within a single wire. In this image, we enhanced the contrast between wire and carbon background for a better visibility of the wire edge.

excitation and probe pulse. Both pulses are overlapped via a dichroic beam splitter and focused (NA 0.9) on the sample. An oil immersion objective (NA 1.3) collects the transmitted light. The pump light is filtered, and the transmitted probe intensity is detected by a photodiode. In addition, we perform luminescence measurements using the same excitation pulses as in the transient absorption measurements. The emitted photoluminescence of the sample is collected in backward direction and guided via flip mirrors into a spectrometer or a single photon counting detector with the possibility of luminescence lifetime measurements. The sample consists of randomly dispersed single nanowires on a glass substrate. High-resolution transmission electron microscopy (TEM) images as presented in Figure 1c give insight in the geometric properties. The diameter is typically between 8 and 14 nm (see Supporting Information) and can be considered as constant for large parts of the wire. However some sections, as imaged in Figure 1d, show fluctuations of the diameter within an individual wire.

We obtain spectral transient transmission data with a temporal resolution of 250 fs by scanning the pump–probe delay for probe wavelengths in 10 nm steps. The pump and probe polarization is along the wire axis. Figure 2 shows an

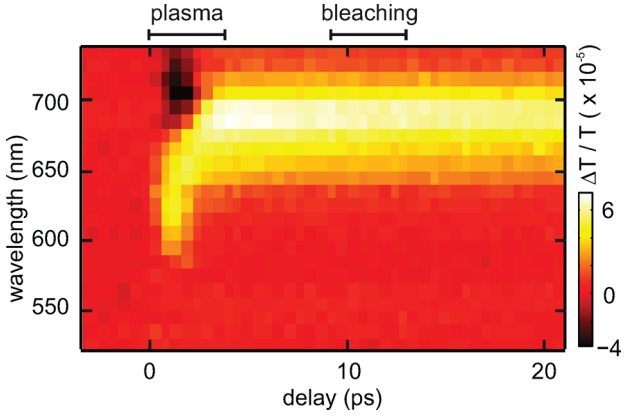

Figure 2. Transient absorption spectra as a function of time delay between pump and probe measured on a single CdSe nanowire with a diameter of 11.6 nm. The zero delay position was corrected for the dispersion in the setup. Two effects on different time scales are observed: An electron–hole plasma leads to a dispersive feature around zero delay, and a pump-induced bleaching of exciton states leads to an absorptive line shape at later times.

example of transient absorption spectra for a single nanowire with a diameter of 11.6 ± 1.5 nm as determined by AFM. We observe relative transmission variations $\Delta T/T$ on the order of some 10^{-5}. Positive transmittance changes (yellow) correspond to a pump-induced decrease of absorption in the wire, and negative transmittance changes (black) correspond to an increase of the absorption. At negative time delays, when the system is probed before the pump excitation, we find no changes in the transmittance for the whole spectrum. This proves the excitation of an undisturbed system and full relaxation until the next pump pulse arrives after 13 ns. Directly after excitation (delay 0 ps) we observe a significant signal ranging from 570 to 740 nm with a dispersive line shape. This feature disappears on a picosecond time scale and changes into a slowly varying absorptive line shape with a maximum at 685 nm wavelength. In the following we will discuss both phenomena in detail. We will attribute the fast feature to an electron–hole plasma and the slow feature to bleaching of excitonic transitions.

Each pump pulse creates many electron–hole pairs due to the large absorption of the nanowire at a wavelength of 390 nm. Using numerical simulations (see Supporting Information) we calculate the absorption cross section of a nanowire with 12 nm diameter and bulk CdSe dielectric properties to 6600 $nm^2/\mu m$ for a polarization along the wire axis. For our pump spot size we obtain approximately 400 absorbed photons per pump pulse, corresponding to an electron–hole density of 10^{19} cm^{-3}. This electron–hole plasma leads to a renormalization of the band gap energy, causing a variation of the complex refractive

dx.doi.org/10.1021/nl400259f | Nano Lett. 2013, 13, 1706–1710

index as a function of carrier density, as observed in wires of larger diamter.[31,32] We observe (Figure 3a) a rising dispersive signal within the first picosecond.[31] In the following three picoseconds a transition from the dispersive to the absorptive line shape takes place. In contrast to wires of larger diameter,[31] in our case the strong confinement seems to cause a faster decay of the plasma. Finally for times >4 ps no further fast changes are found, and the remaining carriers are relaxed in confined states leading to a bleaching of dipole allowed transitions within the wire.

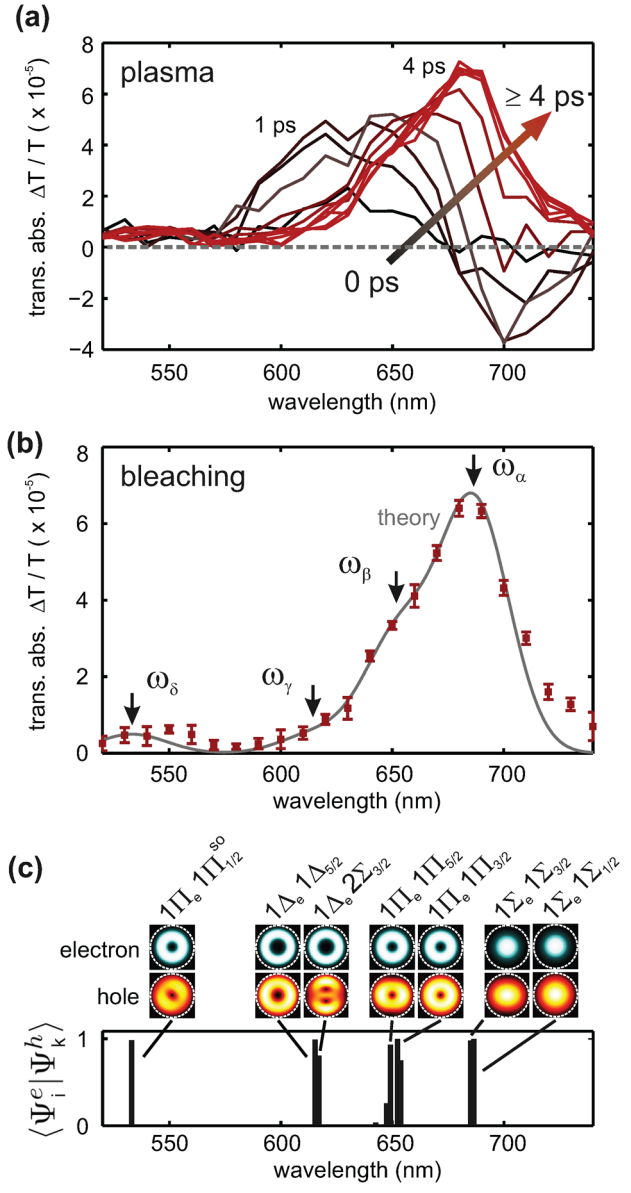

Figure 3. (a) Transient absorption spectra of the section labeled "plasma" in Figure 2. The spectra show the build-up and decay of the dispersive feature due to the electron–hole plasma. The line color encodes the pump–probe delay ranging from black (0 fs) in equal steps of 500 fs until red (7 ps). (b) Averaged transient absorption spectrum of the section labeled "bleaching" in Figure 2 (symbols) as well as the standard deviation over six consecutive measurements (error bars). The gray curve is a fit with four Gaussian at center energies $\omega_\alpha ... \omega_\delta$ (see Table 1), calculated with a six-band effective mass model (wire diameter 11.6 nm). (c) Overlap matrix elements for dipole transitions and the corresponding electron (blue) and hole (red) wave functions for the most probable transitions in the six-band effective mass model. The transitions bunch into four groups.

To interpret the bleaching signal at later delay times, we need to know the eigenenergies of the electron and hole states (levels in Figure 1a) and their transition strengths. We employ a six-band effective mass model, neglecting Coulomb interaction and limiting us to low quantum number states in two dimensions.[13,33] We tune the wire diameter in our simulation to reproduce the position of the lowest energy peak in Figure 3b. The plotted experimental data is the average over the time interval labeled "bleaching" in Figure 2. In the simulations we find a best fitting wire diameter of 11.6 nm, in agreement with our AFM measurements of this wire. Higher energy transitions occur between more complex electron and hole states, bunching together into four effective states, which we label α–δ (see Figure 3c). These four states fully describe our transient absorption signal by only adjusting the amplitudes of four Gaussian lines of equal width (fwhm 37 nm) centered on the calculated eigenenergies. The fit result is shown by the gray line in Figure 3b and summarized in Table 1. The fit amplitudes reflect the pump-induced population of the states, as the overlap matrix elements are almost constant.

Table 1. Four Effective States from the Transient Transmission Spectra in Figure 3, Labeled α to δ[a]

state	α	β	γ	δ
energy (eV)	1.81	1.90	2.01	2.33
wavelength (nm)	685	653	616	533
amplitude (10^{-5})	6.3	3.0	0.6	0.5
$\Delta\sigma$ (nm^2)	7.20	3.10	0.55	0.34
N	30	15	3	3

[a]The peak transient transmission value $\Delta T_{peak}/T$ can be converted into a variation of the absorption cross section $\Delta\sigma$. Assuming single dipoles with a radiative lifetime of 3 ns, we can estimate the number N of states that are filled by each pump pulse.

The integral over an absorption line is connected with the transition dipole moment and the number of dipoles involved.[34,35] This allows us to estimate the number of states that are filled by the pump pulse (see Supporting Information). The result is proportional, via the transition dipole moment, to the assumed pure radiative lifetime τ_{rad} of the emitter. A lower limit is the measured luminescence lifetime. We chose a value of 3 ns, close to the lower limit. This results in about 50 states filled by the pump pulse (Table 1). Distributed over a wire section within the probe focus of approximately 400 nm this would lead to a volume averaged exciton–exciton distance of 12 nm. This is in the order of the exciton Bohr radius of 5.6 nm of bulk CdSe.[17]

In the following we are going to investigate the lifetime of the carrier population. For this purpose we performed delay scans over 400 ps. Figure 4a shows the transient absorption spectra of a wire with a diameter of 7.4 ± 1 nm. The smaller diameter causes a stronger quantum confinement, resulting in a blueshift of the wire response compared to Figure 3. Again we determine the dominant optical transitions in the six-band effective mass model, using a best-fitting wire diameter of 8.2 nm. Here, the β and γ transitions are also blueshifted with respect to the previous wire. The model predicts the δ transition around 500 nm, outside our spectral region. To describe the transient transmission spectra (Figure 4b), we slightly shift the peak positions with respect to the six-band effective mass model

dx.doi.org/10.1021/nl400259f | Nano Lett. 2013, 13, 1706–1710

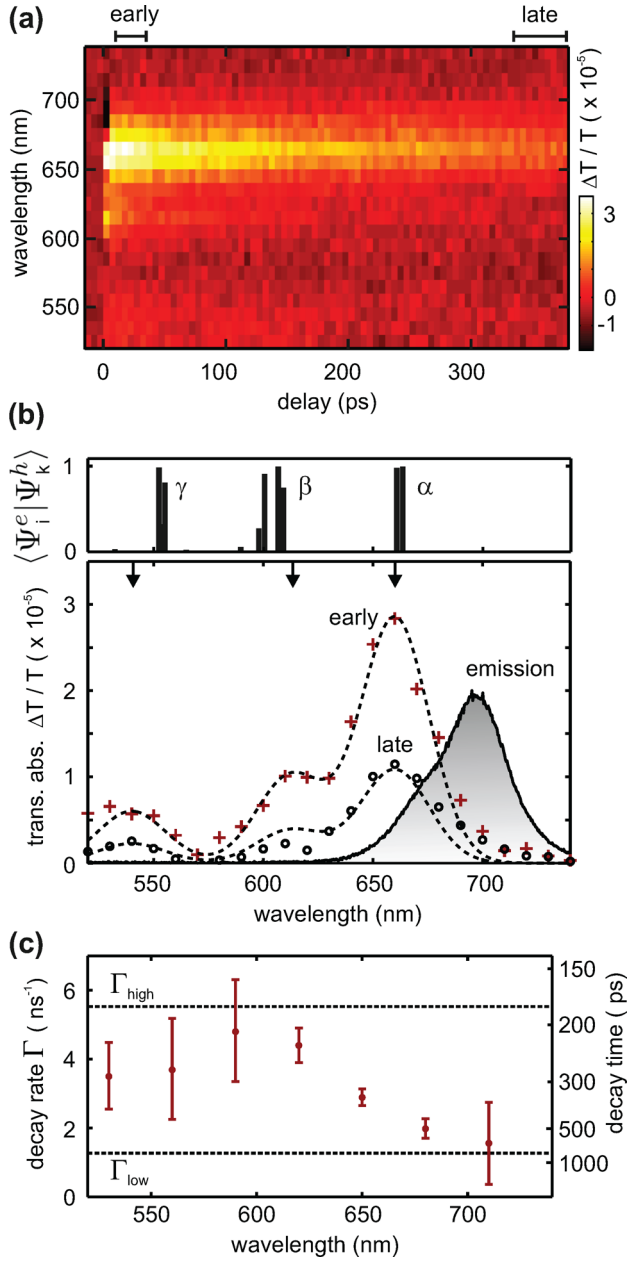

Figure 4. (a) Transient transmission spectra of a different nanowire (diameter 8 nm). (b) Overlap matrix elements for a wire of 8.2 nm diameter (upper graph). Transient transmission spectra averaged over the "early" time interval (red crosses) and the "late" interval (black circles) as marked in panel a. At early times, the data is described by a sum of three Gaussians, indicated by the arrows. At later times, the spectral shape almost does not change, as the same model fits the data after scaling with a single constant. Luminescence emission occurs at about 40 nm red of the absorption peak, where only little transient absorption is measured. (c) Spectral dependence of the decay rates found in the transient transmission data, by averaging over 30 nm spectral width and fitting a single exponential decay. The error bars give the interval over which χ^2 increases by 10%. For comparison, the two dominant components of the luminescence decay, Γ_{low} and Γ_{high}, are given.

(arrows in Figure 4b). We find an overall agreement both for early (10 ps) as well as for late (380 ps) times, using only an amplitude scaling factor between both. The temporal dynamics is thus in first approximation spectrally constant. A single exponential fit to the delay traces gives decay rates between about 2 ns^{-1} around 700 nm and 5 ns^{-1} around 600 nm (Figure 4c).

It is instructive to compare these findings with the luminescence properties of this wire. As the Einstein coefficients are identical for absorption and spontaneous emission, we measure the same process by transient absorption and luminescence emission spectroscopy. By transient absorption we find the number of pump-induced excitations in a state, by emission the number of photons generated from this state. The luminescence emission peak around 700 nm is approximately 40 nm (100 meV) red of the transient absorption peak (Figure 4b). We find a long wavelength tail in the transient absorption spectrum that covers the luminescence emission. Time-resolved spectroscopy of these states gives a decay rate close to the slow component Γ_{low} of the luminescence decay (see Supporting Information). However, the decay rate of the strong α peak does not differ much. We expect thus only little population transfer from the α peak into lower lying emitting states, as this transfer would increase the decay rate. The majority of the nanowire thus leads to a strong transient absorption signal (α peak), but only a weak shoulder in the luminescence spectrum. Some low energy states, which are present in the nanowire only at low density, cause the largest part of the emission. These low energy states could be defect states, fluctuations in the nanowire diameter, or states that include a phonon. The TEM image (Figure 2d) shows short intervals of larger diameter, that is, less confinement.

Comparing excitation and emission rates yields further insight. As discussed above, about 400 photons are absorbed out of each pump pulse. After relaxation about 50 excitons are created, of which about 30 are found in the α peak. The radiative lifetime of τ_{rad} = 3 ns assumed above implies a luminescence quantum efficiency of about 25%, as we measure a luminescence lifetime of about 0.8 ns. We would thus expect about 8−12 emitted photons per laser pulse. Note that this number is independent of the assumed radiative rate, as it cancels out via the quantum efficiency. However, only about 0.02 photons are found in the optical far-field (1.5×10^6 per second), taking into account our detection efficiency of 1.5%. Only one out of 500 emitted photons reaches the far-field. A much lower quantum efficiency of the emitter cannot explain our data, as it would entail a very short excited state lifetime, which is in contrast to our measurements.

We propose reabsorption as cause for the low emission intensity of the nanowire. After emission, the photon is reabsorbed by other parts of the nanowire. From the ground state absorption of the nanowire[13] we estimate about 20 000 absorbing dipole emitters per micrometer wire length for the α peak. In the near surroundings of the excited dipole, Coulomb interaction will shift the states out of resonance. Short distance Förster type energy transfer is thus not possible. Indeed, Förster energy transfer would also modify the decay rate, which is not what we find. Longer distance transfer of the excitation on the wire by reabsorption of the emitted photon then increases the overall probability of nonradiative recombination. To support this model we simulated numerically an emitting dipole within a CdSe nanowire of 400 nm length and 12 nm diameter, using bulk optical properties (see Supporting Information). Within 5.6 nm from the emitter, the wire is assumed being not absorptive due to Coulomb interaction. We find that reabsorption exceeds emission into the far-field by about a factor of 400. This simple model agrees well with the

dx.doi.org/10.1021/nl400259f | Nano Lett. 2013, 13, 1706−1710

experimentally found mismatch between expected and detected photon rate.

In summary, we presented the first time-resolved ultrafast nonlinear spectroscopy of the exciton dynamics in individual CdSe nanowires of diameters well below 20 nm. Single particle spectroscopy removed the inhomogeneity of the nanowire sample, for example, in the wire diameter. The first picoseconds after excitation are dominated by an electron−hole plasma, leading to a dispersive line shape of the transient signal. At later times, we found clear peaks in the transient absorption spectra, indicating a bleaching of excitonic states. The population of these states decays with spectrally rather independent rates between 2 and 5 ns^{-1}. We find a large mismatch between the number of pump-induced excitations of the emitting state (about 10 per laser pulse) and the luminescence photon rate (about 0.02 per laser pulse). Numerical simulations of the power flow of an emitting dipole in a CdSe nanowire reveals that the mismatch is caused by reabsorption of emitted photons by other parts of the nanowire. Emission from low energy defect states is much less absorbed than emission from the nanowire itself. The former thus dominates the emission spectrum, and the latter reduces the overall external quantum efficiency. The combination of single wire transient absorption spectroscopy with luminescence spectroscopy allowed us to track the excitation and emission dynamics. We expect this combination to give, in more detailed experiments, further insight in the intricate photophysics of semiconducting nanowires, especially when combined with plasmonic enhancement of weak nonlinear signals.[36,37]

■ ASSOCIATED CONTENT

Supporting Information

Experimental parameters and dispersion correction, comparison between single and aggregate or ensemble measurement, SEM and TEM images and wire diameter statistics, luminescence measurements, number of absorbed photons, number of bleached exciton states, and simulating the ratio between emission and re-absorption. This material is available free of charge via the Internet at http://pubs.acs.org.

■ AUTHOR INFORMATION

Corresponding Author

*E-mail: m.lippitz@physik.uni-stuttgart.de.

Notes

The authors declare no competing financial interest.

■ ACKNOWLEDGMENTS

We thank G.V. Hartland and M. Kuno for the nanowire sample and F. Phillipp for the TEM images. We acknowledge financial support by the German Science Foundation (SPP 1391) and the Baden-Württemberg Stiftung.

■ REFERENCES

(1) Yang, P. D.; Yan, R. X.; Fardy, M. *Nano Lett.* **2010**, *10*, 1529−1536.
(2) Lu, W.; Lieber, C. M. *Nat. Mater.* **2007**, *6*, 841−850.
(3) Piccione, B.; Cho, C. H.; van Vugt, L. K.; Agarwal, R. *Nat. Nanotechnol.* **2012**, *7*, 640−645.
(4) Woggon, U. *J. Appl. Phys.* **2007**, *101*, 081727.
(5) Kempa, T. J.; Cahoon, J. F.; Kim, S. K.; Day, R. W.; Bell, D. C.; Park, H. G.; Lieber, C. M. *Proc. Natl. Acad. Sci. U.S.A.* **2012**, *109*, 1407−1412.
(6) Cho, C.-H.; Aspetti, C. O.; Turk, M. E.; Kikkawa, J. M.; Nam, S.-W.; Agarwal, R. *Nat. Mater.* **2011**, 1−7.
(7) Yan, R. X.; Pausauskie, P.; Huang, J. X.; Yang, P. D. *Proc. Natl. Acad. Sci. U.S.A.* **2009**, *106*, 21045−21050.
(8) Fedutik, Y.; Temnov, V. V.; Schoeps, O.; Woggon, U.; Artemyev, M. V. *Phys. Rev. Lett.* **2007**, *99*, 136802.
(9) Vietmeyer, F.; McDonald, M. P.; Kuno, M. *J. Phys. Chem. C* **2012**, *116*, 12379−12396.
(10) Protasenko, V. V.; Hull, K. L.; Kuno, M. *Adv. Mater.* **2005**, *17*, 2942−2949.
(11) Kulzer, F.; Orrit, M. *Annu. Rev. Phys. Chem.* **2004**, *55*, 585−611.
(12) Myalitsin, A.; Strelow, C.; Wang, Z.; Li, Z.; Kipp, T.; Mews, A. *ACS Nano* **2011**, *5*, 7920−7927.
(13) Giblin, J.; Vietmeyer, F.; McDonald, M. P.; Kuno, M. *Nano Lett.* **2011**, *11*, 3307−3311.
(14) Giblin, J.; Syed, M.; Banning, M. T.; Kuno, M.; Hartland, G. *ACS Nano* **2010**, *4*, 358−364.
(15) Carey, C. R.; LeBel, T.; Crisostomo, D.; Giblin, J.; Kuno, M.; Hartland, G. V. *J. Phys. Chem. C* **2010**, *114*, 16029−16036.
(16) Lupo, M. G.; Della Sala, F.; Carbone, L.; Zavelani-Rossi, M.; Fiore, A.; Lüer, L.; Polli, D.; Cingolani, R.; Manna, L.; Lanzani, G. *Nano Lett.* **2008**, *8*, 4582−4587.
(17) Robel, I.; Bunker, B. A.; Kamat, P. V.; Kuno, M. *Nano Lett.* **2006**, *6*, 1344−1349.
(18) Mohamed, M.; Burda, C.; El-Sayed, M. *Nano Lett.* **2001**, *1*, 589−593.
(19) Htoon, H.; Hollingsworth, J.; Dickerson, R.; Klimov, V. *Phys. Rev. Lett.* **2003**, *91*, 227401.
(20) Carey, C. R.; Yu, Y.; Kuno, M.; Hartland, G. V. *J. Phys. Chem. C* **2009**, *113*, 19077−19081.
(21) Lo, S. S.; Major, T. A.; Petchsang, N.; Huang, L.; Kuno, M. K.; Hartland, G. V. *ACS Nano* **2012**, *6*, 5274−5282.
(22) Puthussery, J.; Lan, A.; Kosel, T. H.; Kuno, M. *ACS Nano* **2008**, *2*, 357−367.
(23) Glennon, J. J.; Buhro, W. E.; Loomis, R. A. *J. Phys. Chem. C* **2008**, *112*, 4813−4817.
(24) Glennon, J. J.; Tang, R.; Buhro, W. E.; Loomis, R. A. *Nano Lett.* **2007**, *7*, 3290−3295.
(25) Brokmann, X.; Coolen, L.; Dahan, M.; Hermier, J. *Phys. Rev. Lett.* **2004**, *93*, 107403.
(26) Biebricher, A.; Sauer, M.; Tinnefeld, P. *J. Phys. Chem. B* **2006**, *110*, 5174−5178.
(27) Yu, H.; Li, J.; Loomis, R.; Gibbons, P.; Wang, L.; Buhro, W. *J. Am. Chem. Soc.* **2003**, *125*, 16168−16169.
(28) Giblin, J.; Protasenko, V.; Kuno, M. *ACS Nano* **2009**, *3*, 1979−1987.
(29) Giblin, J.; Kuno, M. *J. Phys. Chem. Lett.* **2010**, *1*, 3340−3348.
(30) Zhang, J.; Lutich, A. A.; Rodriguez-Fernandez, J.; Susha, A. S.; Rogach, A. L.; Jaeckel, F.; Feldmann, J. *Phys. Rev. B* **2010**, *82*, 155301.
(31) Montazeri, M.; Jackson, H. E.; Smith, L. M.; Yarrison-Rice, J. M.; Kang, J.-H.; Gao, Q.; Tan, H. H.; Jagadish, C. *Nano Lett.* **2012**, *12*, 5389−5395.
(32) Banyai, L.; Koch, S. *Z. Phys. B-Condens. Matter* **1986**, *63*, 283−291.
(33) Shabaev, A.; Efros, A. *Nano Lett.* **2004**, *4*, 1821−1825.
(34) Loudon, R. *The Quantum Theory Of Light*; Oxford University Press: New York, 2000.
(35) Strickler, S.; Berg, R. *J. Chem. Phys.* **1962**, *37*, 814.
(36) Schumacher, T.; Kratzer, K.; Molnar, D.; Hentschel, M.; Giessen, H.; Lippitz, M. *Nat. Commun.* **2011**, *2*, 333−335.
(37) Pfeiffer, M.; Lindfors, K.; Atkinson, P.; Rastelli, A.; Schmidt, O. G.; Giessen, H.; Lippitz, M. *Phys. Status Solidi B* **2012**, *249*, 678−686.